This article was published in Powder Technology, 272, 14-22, 2015

http://dx.doi.org/10.1016/j.powtec.2014.11.016

Cyclone optimization including particle clustering

André Alves [a], Julio Paiva [a,*], Romualdo Salcedo [a,b]

[a] Advanced Cyclone Systems S.A., Porto, Portugal

[b] LEPABE, DEQ, Faculdade de Engenharia da Universidade Porto, Porto, Portugal

Abstract

In this work, a new family of geometries of reverse-flow cyclones was obtained through numerical optimization, using a stochastic random search global optimizer coupled with the PACyc model. The objective was to optimize the geometry of a reverse-flow cyclone taking into account inter-particle agglomeration (clustering), since this phenomenon usually occurs to some degree in industrial cyclone operation, increasing the collection of fine particles.

Experimental results for three kinds of particles and particle size distributions are shown using a pilot-scale unit. An industrial implementation of the new optimized cyclone is described and the results concerning the performance of the system are shown and compared with predictions from the PACyc model.

The results show a highly improved global efficiency when compared to that of a cyclone geometry obtained by a similar optimization methodology while neglecting the agglomeration/clustering effect. This opens the possibility of using reverse-flow cyclones to capture very fine particles, complying with strict emission limits, such as those from biomass boiler exhausts.

1. Introduction

Cyclones are gas–solid separation devices used in a wide variety of industries and for several purposes, such as for the recovery of raw and process materials, as collectors to reduce the atmospheric pollution complying with particle emission limits, as primary collectors to decrease the burden on more expensive secondary collectors or as particle size classifiers. Cyclones are well known to be able to operate under a wide variety of conditions, including at high temperatures and/or at high pressures, and are characterized by low investment and operating costs.

Typical reverse-flow cyclones are associated with low efficiency for small particles (<5 μm), but previous work [1–10] has shown that this effect may be minimized using numerically optimized cyclones. In spite of this optimization, for fine and low-density particles, the non-ideal effect of re-entrainment may occur, being justifiable both by the smaller aerodynamic diameter of the particles and also for too high inlet velocities for a given geometry [1,4,11,12]. This non-ideal effect may decrease collection efficiency below theoretically predicted values.

The main objective of this work is to describe the development of a new numerically optimized cyclone, the Hurricane_MK, capable of taking into account the agglomeration/clustering effect, always trying to maximize the overall efficiency, while maintaining the re-entrainment effect within reasonable limits. This paper describes the development process of this new range of geometries, the results of the experiments performed in a pilot-scale unit for one such geometry using three different kinds of particles (referred to as samples A, B and C), all commonly found in industrial applications, and a case describing the implementation of the Hurricane_MK at industrial scale.

2. Modeling and optimization

The geometry of a typical reverse-flow cyclone is shown in Fig. 1, where the main geometric variables used to completely define the cy-clone are given. For the posed numerical optimization problem, all these variables are used as decision variables.

In order to make an easier comparison between different sized cy-clones, the cyclone geometry is defined by the ratio of each dimension to the cyclone diameter D. Taking this dimensionless approach, several geometries were developed [5,13–17] based both on empirical development as well as on mathematical models.

2.1. Cyclone optimization theoretical background

Focusing on the improvement of cyclone performance (e.g. maximizing global efficiency), previous work was done in order to develop and optimize the geometry of reverse-flow gas cyclones through numerical optimization [4–7].

Many authors have recently resorted to CFD studies for partial cy-clone optimization, however, to our knowledge, the CFD approach has not yet been used for full cyclone optimization, due to the very large computational burden, as the flow is highly vorticial, assimetric and multiphase with polidispersity. With stochastic global search algorithms, we have shown that this is feasible in usable time and effort [4].

Salcedo [4,8,10] developed an optimized cyclone geometry, combining the MSGA stochastic optimization algorithm [18], with a classical numerical model to predict cyclone performance [19].

Briefly, the MSGA stochastic algorithm used in this work, is an adaptive random search algorithm able to cope with non-convex NLP and MINLP problems, that keeps a guided track of the history of the optimization. Convergence of stochastic algorithms can only be given as a probability in reaching the global optimum, thus sever-al runs have to be made from different starting points, constraint limits and random trial sizes. The MSGA algorithm has been used to solve complex nonlinear NLP and MINLP problems, with a high rate of success in reaching the global optimum [20–22]. The interested reader may consult the above references for a better grasp of the algorithm capabilities.

The set of obtained geometries — the RS_VHE cyclone [1,4,8,9] —was experimentally proven at laboratory, pilot and industrial scales to be more efficient than other high-efficiency geometries for a wide range of experimental conditions, and for several kinds of processes.

This optimized geometry (currently renamed Hurricane cyclone) obeys several constraints, such as maximum allowable pressure drop [15,23–28], saltation velocity [12] and geometrical considerations (as referred by the group of equations (Eqs. (2)–(11))). The objective function used in this optimization was the maximization of global collection efficiency as given by the PACyc model [29],

$$f_{obj} = \max(\text{global collection efficiency}) \quad (1)$$

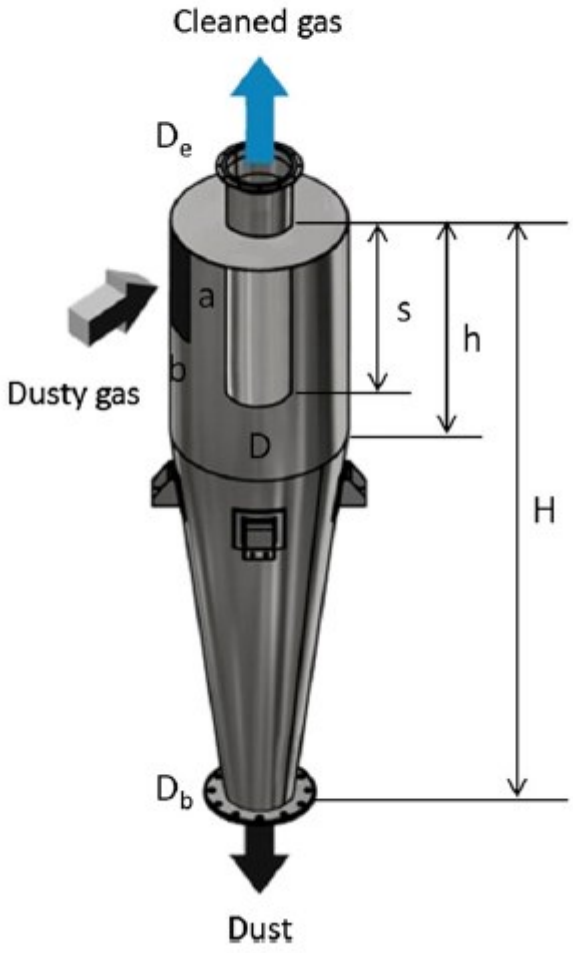

Fig. 1. Typical reverse-flow cyclone

for a defined set of operation conditions and particle size distributions and the following inequality constraints.

$$\Delta P \leq \Delta P_{max} \quad (2)$$

$$6.8^{\circ} < e < 16^{\circ} \quad (3)$$

$$0.5 < \frac{4ab}{\pi D_e^2} < 0.735 \quad (4)$$

$$\frac{u_{in}}{u_s} < 1.25 \quad (5)$$

$$s < h < H \quad (6)$$

$$0.5D_e < D_b < D_e \quad (7)$$

$$0.5(D - D_e) > b \quad (8)$$

$$s > 1.25a \quad (9)$$

$$2.3D_e\left(\frac{D^2}{ab}\right)^{\frac{1}{3}} < H - s \quad (10)$$

$$u_s = 4.912\left(\frac{4g\mu\rho_p}{3\rho}\right)^{\frac{1}{3}}\left[\frac{\left(\frac{b}{D}\right)^{0.4}}{\left(1-\left(\frac{b}{D}\right)^{\frac{1}{3}}\right)}\right] D^{0.067} u_{in}^{\frac{2}{3}}. \quad (11)$$

A detailed explanation of these equations can be found elsewhere [4, 30]. The classical model used in the optimization to calculate the grade-efficiency was the Mothes and Löffler [19] model which depends on an empirical parameter (D_{turb} — particle turbulent dispersion coefficient). This was studied by Salcedo and Coelho [31] and coupled to the model to confer it with predictive capabilities, as this parameter was found to depend on particle size distribution, operating conditions and cyclone geometry.

2.2. Agglomeration/clustering in cyclones

The Hurricane cyclone has shown consistently good results when applied to very different dusts both at pilot and industrial scales [1,9, 29,32,33]. Many experimental results showed abnormal high collection for very fine particles (<1–2 μm), a characteristic that none of the classical models for gas cyclones, such as Mothes and Löffler [19], was able to predict.

Paiva et al. [29] developed a model to explain this behavior, following the original thoughts of Mothes and Löffler [34] that particle ag-glomeration due to interparticle collision was the culprit, thus having a key role on the cyclone' overall performance.

This hypothesis led to the PACyc model [29], with the main purpose of obtaining simultaneously more accurate and robust predictions for cyclone efficiency. By employing a fixed set of parameters proposed by Ho and Sommerfeld [35] and by Gronald and Staudinger [36], later fine-tuned by Paiva et al. [29], the model determines if a particle collision occurs and when so, if a particle cluster forms.

The collision effect is affected by each particle size (and correspondingly by its mass and energy) and it is expected that the smaller particles tend to collide with higher probability with the large ones, since their relative velocity will be larger than that for similar sized particles. If the particle energy is too high, the amount of available energy after collision will be enough for the particles to split apart, not forming a particle cluster. Thus, denser particles are less prone to agglomerate.

Finally, if all the favorable conditions are obeyed, a cluster (or agglomerated particle) is formed, and the initial particles (probabilistically one small and one large) will have a dynamic behavior inside the cyclone as a larger particle. The collection of an agglomerated/clustered particle will be different from that of the original particles, thus justifying the increased collection for the smaller particles.

Therefore, PACyc leads to a better prediction of the experimental grade-efficiency curves and in particular of the overall collection. The major drawback is that of a large computational burden, since a probabilistic analysis is built based on the combinatorial random particle collision rate. In order to make a realistic sampling of the original particle size distribution entering the cyclone, while keeping the computational burden at a realistic level, simulations with 300–500k particles lead to results (overall) within a good approximation of the experimental data. CPU times for an Intel Core i7 @ 3.4 GHz are, on average, about 18 h for sampling 300k particles, but depending on the particle size distribution, may take much longer.

This computation burden is a consequence to the fact of all the particles being injected in a combinatorial way, where the binary interactions are randomly analyzed in each time step, updating the fluid velocity and the particles' positions until the final time of interaction is reached. This value is defined by the combination of geometrical and operation data. PACyc implements two additional simplifications to avoid CPU and memory insufficiency: maintaining the number proportion among classes (assigning a single particle to the class with the smallest number of particles), using one of two different strategies: either defining the maximum injected diameter in the control volume (defined as the cut-off diameter) or else defining the number of representative particles through a random sampling. In all these results, the later strategy was used, and further details are presented in Paiva et al. [29].

2.3. New optimized cyclone

The optimization approach was performed using the stochastic adaptive random search global optimizer MSGA [18], as referred above, which is on one hand justified by the numerical complexity of the problem (leading to an ill-conditioned and stiff problem), and also o the fact that stochastic methods are more robust, albeit the drawback of longer execution times.

2.3.1. Problem solving numerical strategy

Having two different sets of tools, one for optimization and the other for simulation with better predictive capabilities, the next step was to couple them to obtain a new optimized cyclone geometry, where the agglomeration effect could be taken into account.

Considering the constraints in terms of computer times, Fig. 2 shows the adopted strategy that allowed the authors to obtain coupled simulation/optimization results in fesible times.

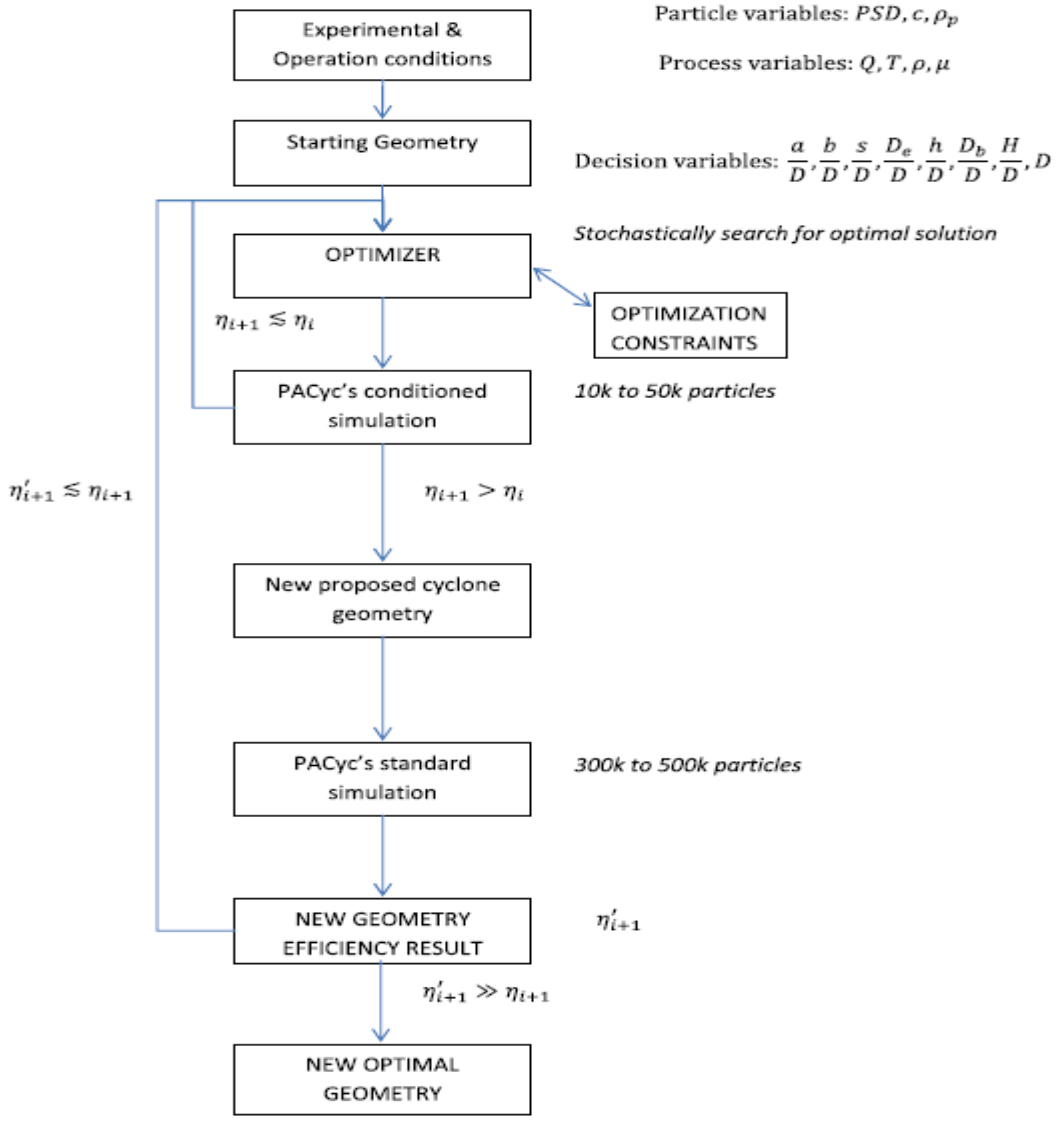

Fig. 2. Optimization flow sheet

Starting from a defined set of conditions related to the particles (particle size distribution — PSD, concentration — c [kgp/mf^3], particle density — ρ_p [kg$_p$/m^3_p], etc) and operation conditions (flow rate — Q [m^3_p/h], temperature — T(°C),fluid's density — ρ [kg$_f$/m^3_f], fluid's viscosity — μ [kg/m·s], etc) and defining a starting cyclone geometry (based on the standard ratios used to define a cyclone), the optimizer runs a con-ditioned PACyc simulation, with much less injected particles (10k to 50k) than a standard one (300–500k) comparing the results with the set of optimization constraints. After having a feasible cyclone geometry that leads to a better performance (η_{i+1}) than the previous (η_i), a standard PACyc simulation is run, to obtain the effective efficiency (η'_{i+1}). If the latter is marginally better than the previous one (η_{i+1}), a new optimization process starts. If the latter is significantly better that the previous one, i.e.,

theoretically reducing emissions by at least 50%, a new cyclone geometry is considered to have been successfully obtained.

2.3.2. Constraint fine tuning

The empirical correlation to determine the saltation velocity, referred in Eq. (5), and obtained by Eq. (11), may not be of general applicability and/or valid for all cyclone geometries.

Previous work by Salcedo and Candido [4] used the constraint on saltation velocity to obtain the Hurricane cyclone in order to minimize the re-entrainment phenomenon. Thus, in the present work the constraint, while considered in the model, was partially relaxed for the optimization of the new cyclone.

At the time of the Hurricane optimization, due to the absence of a general pressure drop model, several models were used (Shepherd and Lapple [23], Caplan [24], Bohnet and Lorenz [25], Dirgo and Leith [15],Barth [26], Stairmand [27],Muschelknautz [28]), and the optimiza-tion was performed, to have a safety margin, using the highest value for the theoretical pressure drop from all these models. In the present work, a new general correlation by Chen and Shi [37] for pressure drop in cyclones was considered, as it has been shown by these authors to be of wide applicability and sufficient accuracy, also accounting for the effect of particle concentration on pressure drop.

3. Results of pilot scale and industrial experiments

An optimized 460 mm i.d. diameter Hurricane_MK was built, and several experiments were done at pilot-scale, with the major results shown below. The pilot test rig is shown in Fig. 3a and b.

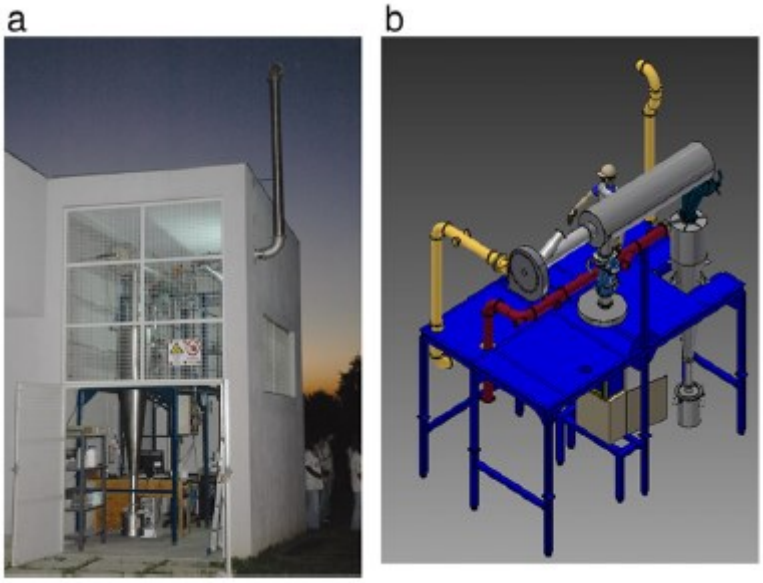

Fig. 3. a. Pilot test rig. b. 3D representation of the pilot test rig.

Due both to a patent pending process [38] and to commercial sensitivity, the geometry of the Hurricane_MK cannot be disclosed. However, it is characterized by a large cylinder-to-cone length ratio, and by a relatively narrow gas entry and a narrow gas exit.

All the experiments were performed at a pilot test rig with sampling locations at the inlet and outlet of the pilot cyclone. A TOPAS 410G particle feeder was employed at different rates for each experiment and the grade-efficiency curves were obtained through simultaneous inlet/outlet isokinetic samplings using constant volume samplers (Techora Bravo), combined with GFA glass fiber filters. The particle size distributions were obtained off-line with a laser diffraction particle size analyzer (Coulter LS230). Finally, the theoretical results were obtained through PACyc, using either the average experimental operating conditions or a representative condition. For the sensitivity of PACyc to inlet concentration, the reader is referred elsewhere [25].

The experiments were performed with a flow rate of ambient air of 311 m^3/h at temperatures between 15 and 30 °C, leading to a cyclone pressure drop of 1.95 ± 0.15 kPa. For these conditions, the Chen and Shi [37] model predicts pressure drops between 1.85 and 2.05 kPa. Three kinds of particles and particle size distributions were chosen to test the performance of the Hurricane_MK (referred as samples A, B and C), representing dusts with industrial relevance.

Sample A particles are very difficult to capture by regular cyclones and multicyclones mainly due to their small size and high porosity. Since these particles were already tested with the Hurricane cyclone, at similar pressure drop, it was possible to establish a direct comparison between the behaviors of the two cyclone geometries.

Sample B particles were obtained from the catch of a mechanical ReCyclone® system from a wood-waste biomass boiler, thus with high relevance for full-scale applications. Common high-efficiency cy-clones and multicyclones are not able to reduce these boiler emissions below about 150–300 mg/Nm^3, and sometimes only to much larger values [8].

Regarding sample C, the particles were tested in this work in order to study the efficiency of this cyclone for nanoparticle capture, a field where Hurricane cyclones coupled in electrostatic recirculation loops have already shown surprisingly good results. Apart from their small size, these particles are extremely porous, representing a very difficult case to any mechanical dry deduster.

The particle density is a very important parameter to include in any cyclone modeling for predicting collection efficiency. The densities presented in this work were found using the combination of two methods: helium picnometry to obtain true particle density (the particle volume excludes intraparticle and interparticle pores); mercury picnometry to obtain the apparent density (the particle volume without mercury penetrating the micro and mesopores, thus obtaining the total volume of the particle, including the intraparticle but excluding the interparticle volumes). Mercury picnometry corresponds to the preparative part of mercury porosimetry, limiting applied pressure to about 2 kPa, to simultaneously avoid mercury penetration into the intraparticle pores and to guarantee that the interparticle spaces are occupied.

The PACyc model uses the apparent density as obtained by Hg picnometry as the representative particle density.

Table 1 shows the properties of samples A, B and C in terms of density and porosity where ρ_p is the real density, ρ_{ap} is the apparent density and ε is the porosity. Real density was measured by He picnometry, and apparent density by Hg porosimetry.

All the cases are presented following the same structure, with a global discussion in Section 4.

Table 1. Properties of the samples used in the experimental tests.

Sample	ρ_p (kg/m^3)	ρ_{ap} (kg/m^3)	ε
A	2379	906	0.62
B	2443	1014	0.59
C	5310	1570	0.70
Industrial	2233	832	0.66

Table 2 presents the global efficiencies for all the experiments performed (pilot and industrial scale), theoretical global efficiencies obtained with PACyc and the global efficiency of the Hurricane cyclone (HR) for the same particles, at similar pressure drop. In Table 2,C_{in} is the inlet concentration and C_{out} is the outlet concentration, where η is the global efficiency.

We include 4 different cases, because it has recently been found [39] that cyclones may behave differently with dusts of similar size and density, depending on their tendency to agglomeration or to attrition.

Table 2. Global efficiencies.

Case ID	Run	C_{in} (mg/m^3)	C_{out} (mg/m^3)	$\eta_{experimental}$ (%)	$\eta_{theoretical}$ (%)
Pilot — sample A	1	84	8	90.5	–
	2	450	33	92.7	–
	3	584	40	93.2	–
	PACyc_MK	429	–	–	92.0
	PACyc_HR	161	59	62.1	60.4
Pilot — sample B	1	121	6	95.1	–
	2	363	15	95.8	–
	3	1231	43	96.5	–
	PACyc_MK	572	–	–	96.3
	PACyc_HR	121	–	–	81.1
Pilot — sample C	1	362	74	79.6	81.9
Industrial	Exp	1048[a]	94[a]	91.0	90.0

[a] At NTP conditions, dry, 11% O_2.

3.1. Case 1 — sample A

Three experiments with very fine particles (median volume diameter of about 2.5 μm with 32% <μm) were done with different inlet concentrations in order to evaluate the efficiency of the Hurricane_MK for this kind of particles. The particle size distribution that was fed to the pilot cyclone is shown in Fig. 4.

Fig. 5 compares the experimental and theoretical grade efficiencies as a function of particle diameter.

Fig. 6 presents the outlet particle size distributions for two of the experiments with a median volume diameter of about 0.4 μm and 90% <1 μm.

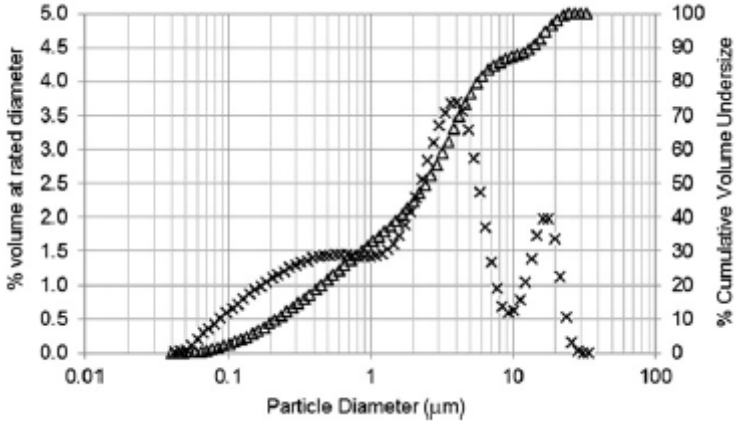

Fig. 4. Particle size distribution in feed. The series with the "x" plots the % volume at rated diameter and the series with the "Δ" plots the cumulative volume undersize.

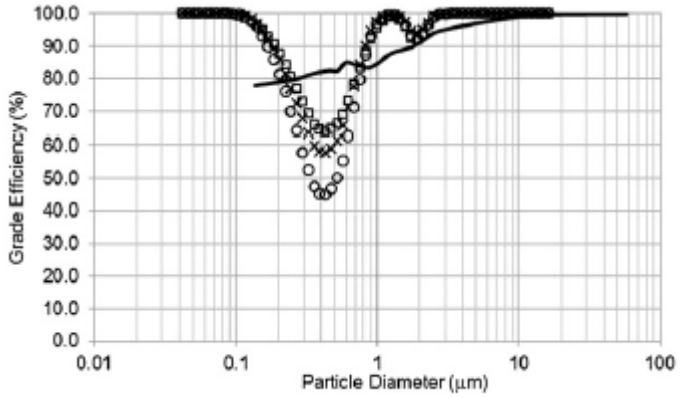

Fig. 5. Theoretical and experimental grade efficiencies. Series with "" plots the grade efficiencies for C_{in} = 84 mg/m^3, series with "x" for C_{in} = 450 mg/m^3, series with the "□" for C_{in} = 584 mg/m^3. The series with solid line plots the PACyc results for C_{in} = 429 mg/m^3.

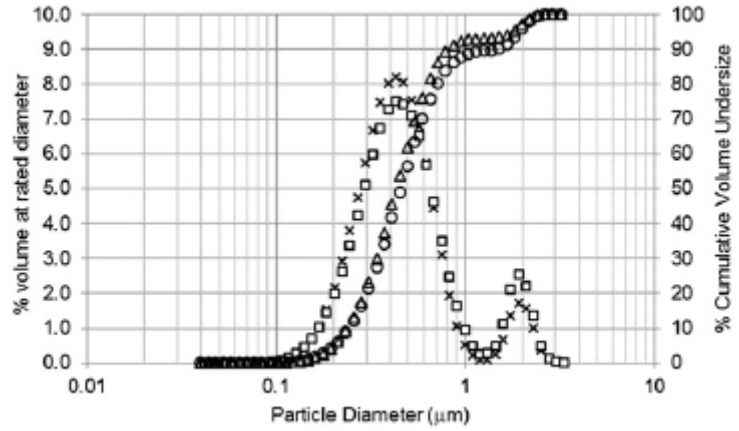

Fig. 6. Particle size distributions at the outlet of the pilot rig. Series with "x" plots the outlet distribution for Cin = 450 mg/m^3, series with "□" for Cin = 584 mg/m^3. Series with "Δ" plots the cumulative undersize distribution in the outlet for Cin = 450 mg/m^3, series with "" for Cin = 584 mg/m^3.

Eq. (12) is the model proposed by Smolik [40] to represent the increase in efficiency due to an increase in the inlet concentration:

$$\eta(C_2) = 1-(1-\eta(C_1))\left(\frac{C_1}{C_2}\right)^k. \qquad (12)$$

The Smolik model allows the prediction of efficiency for a given concentration (C_2) knowing the efficiency at a lower value (C_1). The empirical constant proposed by Smolik is k = 0.18 but it is problem dependent, so it must be adjusted for any particular case. In other words, particles may increase collection with increased inlet concentration to a different level than that given by the k = 0.18 factor.

For the case of sample A, the adjusted value of k was 0.163 (Fig. 7), meaning that this dust increases its collection efficiency with the in-crease in inlet concentration to a similar degree than expected from the Smolik experimental exponent.

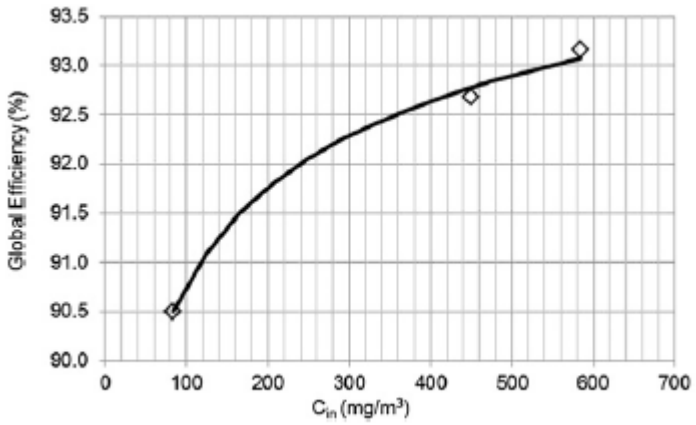

Fig. 7. Series with "□" plots the experimental global efficiencies in function of the inlet concentration and the series with solid line plots the global efficiencies obtained through the Smolik model with k = 0.163.

3.2. Case 2 — sample B

Three experiments were performed at different inlet concentrations with this specific sample, consisting of ashes from a wood-waste bio-mass boiler obtained from a mechanical ReCyclone® [32],placeddown-stream from a low pressure drop cyclone acting as a primary deduster. The particle size distribution at the inlet of the optimized Hurricane_MK cyclone given in Fig. 8 shows fine particles (median volume diameter about of 5 μm with 9.8% <1 μm).

Fig. 9 presents the theoretical and experimental grade efficiency curves for the three experiments, where the PACyc simulation was built based on the average experimental concentration.

Fig. 10 presents the particle size distributions of the cyclone emissions, having a median volume diameter about of 2.7 µm and 15% <1 µm.

The Smolik's fit was built for this case, giving an adjusted k = 0.141.

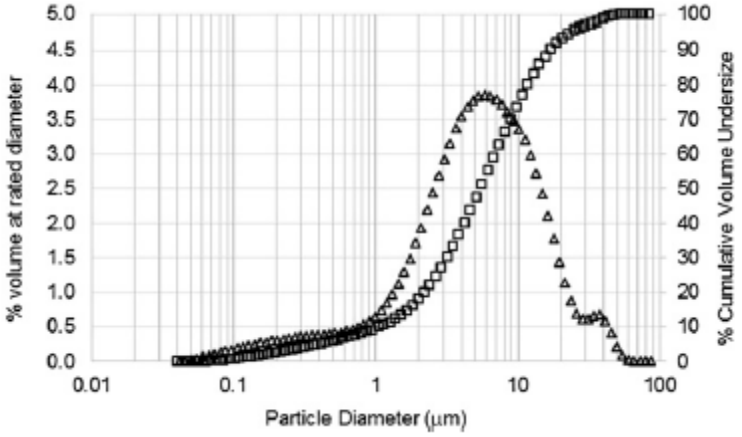

Fig. 8. Particle size distribution in feed. Series with "Δ" plots the % volume at rated diameter and series with "□" plots the cumulative volume undersize.

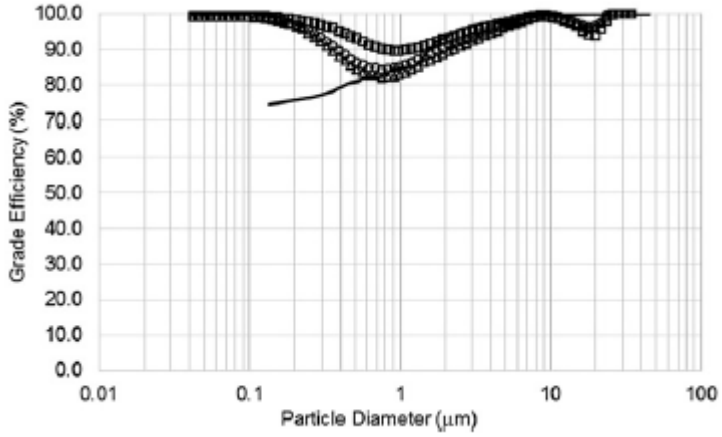

Fig. 9. Theoretical and experimental grade efficiencies. Series with "Δ" for Cin = 121 mg/m^3 , series with "" for Cin = 363 mg/m^3 , series with "□" for Cin = 1231 mg/m^3 and series with solid line plots the PACyc results for Cin = 572 mg/m^3.

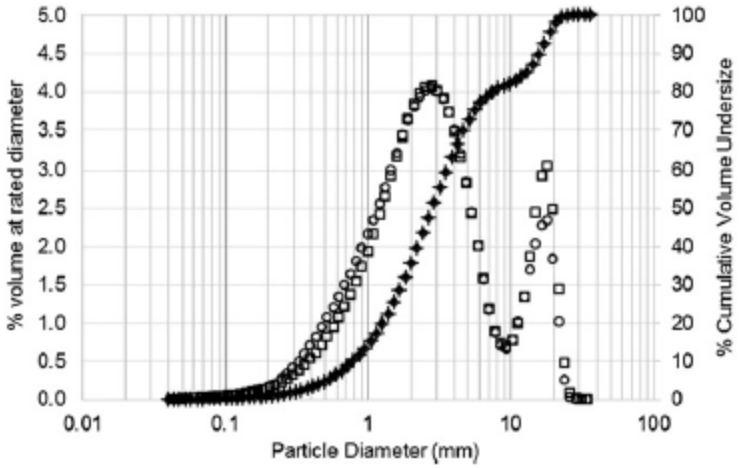

Fig. 10. Particle size distribution at the outlet of the pilot rig. Series with "" plots the outlet distribution for Cin = 363 mg/m^3, series with "□" for Cin = 1231 mg/m^3. Series with "+" plots the cumulative volume undersize for Cin = 363 mg/m^3, series with "◊" for Cin = 1231 mg/m^3.

3.3. Case 3 — sample C

One experiment was performed with very fine particles, with median volume diameter of about 1.1 μm and 40% <1 μm (seeFig. 12). Furthermore, the particles are highly porous (≈70%), representing a very difficult case for any reverse-flow cyclone.

Superimposed in Fig. 13 are the experimental and theoretical grade efficiencies for this case.

Fig. 14 shows the particle size distributions of the cyclone emissions having a median volume diameter about of 0.5 μm and with 99% <1 μm.

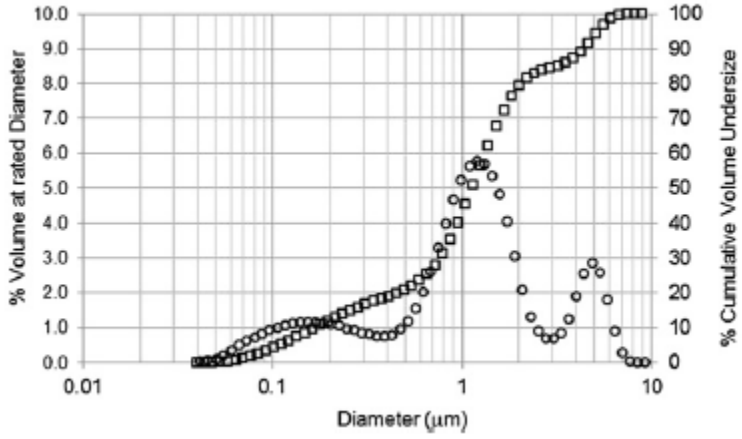

Fig. 12. Particle size distribution in feed. Series with "" plots the % volume at rated diameter and the series with the "□" plots the cumulative volume undersize.

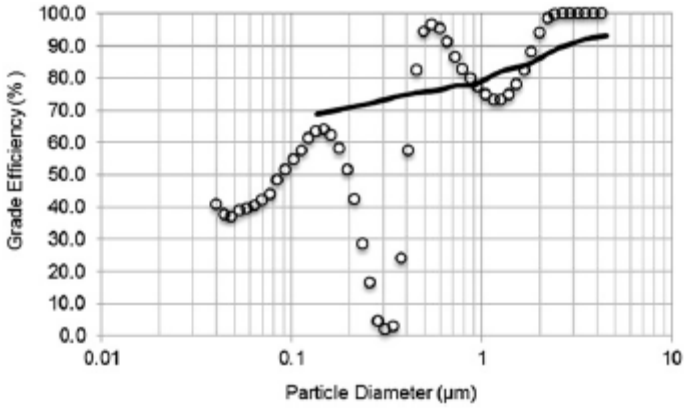

Fig. 13. Theoretical and global grade efficiencies. Series with "" plots the experimental grade efficiencies for Cin = 363 mg/m^3 and the series with the solid line plots the PACyc results for Cin = 363 mg/m^3.

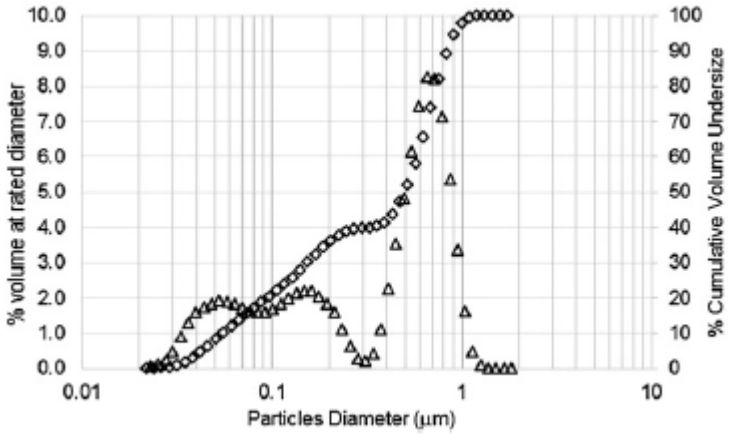

Fig. 14. Particle size distribution at the outlet of the pilot rig. Series with the "Δ" plots the outlet distribution for Cin = 362 mg/m^3. Series with the "◊" plots the cumulative volume undersize for Cin = 362 mg/m^3.

3.4. Industrial application of the Hurricane_MK

A Hurricane_MK system consisting of a parallel array of 24 Hurricane_MK each 1050 mm in diameter, was installed in an industrial facility in order to reduce the emissions from a cork waste biomass boil-er. The operating conditions were 36,525 ± 4625 m3/h @ 163.8 °C with an O2 level of 12.9% (dry basis) and water content of 6.4% by volume.

The objective of this installation is to reduce the emissions after the installed multicyclones by 10-fold, to comfortably comply with the Por-tuguese legal limits (150 mg/Nm3 @11%O2). The system total pressure drop is 1.58 kPa at the operating conditions referred above.

The results were obtained through isokinetic sampling at inlet (out-let of the multicyclones) and outlet of the optimized cyclone system, and the particle size distributions were obtained by

using the same method mentioned above for the pilot-scale experiments. The theoret-ical results were once again obtained through PACyc.

Fig. 15 shows the particle size distribution at the inlet of the system. The particles are fine, having a median volume diameter about of 7.1 µm and 10.6% b1 µm.

Fig. 16 shows the experimental and theoretical grade efficiency curves.

Fig. 17 shows the particle size distributions of the cyclone emis-sions having a median volume diameter about of 2.3 µmand with 20.4% b1 µm.

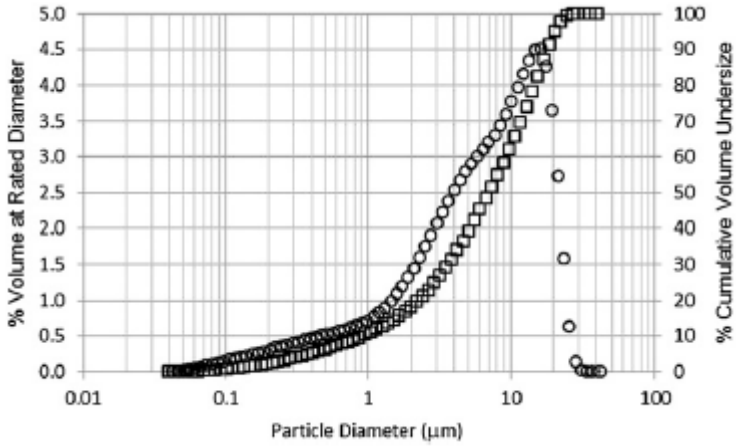

Fig. 15. Particle size distribution in the inlet of the system. Series with "" plots the % volume at rated diameter and the series with the "□" plots the cumulative volume undersize.

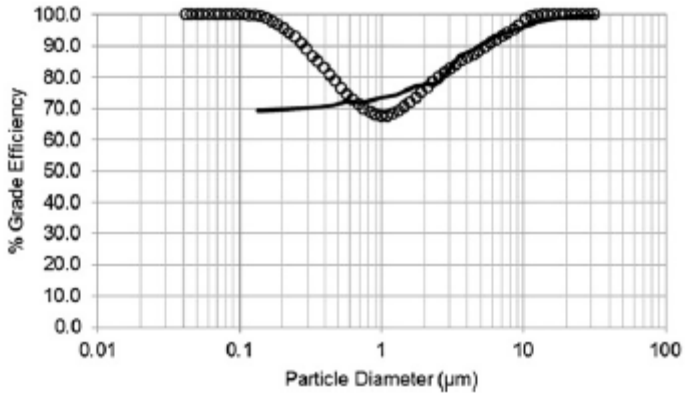

Fig. 16. Theoretical and global grade efficiencies for the industrial case. Series with "" plots the experimental grade efficiencies and the series with the solid line plots the PACyc results.

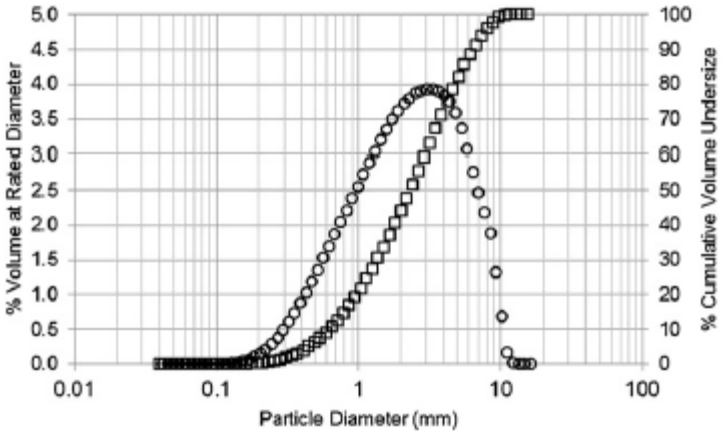

Fig. 17. Particle size distribution at the outlet of the system. Series with the "" plots the outlet and the series with the "□" plots the cumulative volume undersize.

4. Discussion

Since the purpose of this work is to show the applicability of a cyclone geometry obtained by numerical optimization integrating the phenomenon of inter-particle collision/agglomeration/clustering, this section will discuss the combined results of all the experiments and pre-dictions shown above.

4.1. Global efficiency vs. grade efficiency-curves

According to the results obtained (see Table 2), the global efficiency increases with the increase in the inlet concentration. This phenomenon is also observed in the grade efficiency curves (see Figs. 5 and 9) and in the results of the Smolik's fit(see Figs. 7 and 11). Thus, the behavior of the Hurricane_MK is not qualitatively different from any other reverse-flow cyclone, including that of the numerically optimized Hurricane.

4.2. Hurricane_MK vs. Hurricane cyclone

A comparison of the performance between the Hurricane_MK and the Hurricane cyclone was done in case 1 (see Table 2), and in case 2 only theoretically. For inlet concentrations between 84 and 450 mg/m3,global efficiencies between 90.5 and 92.7% were obtained for the Hurricane_MK. One experiment performed with the Hurricane cyclone at similar pressure drop with an intermediate inlet concentration of 161 mg/m3 of the same particles and particle size distribution resulted in an efficiency of 62.1%, so for sample A the Hurricane_MK cyclone is significantly more efficient than the Hurricane. This result is due to the fact, as previously mentioned, that the Hurricane_MK was optimized taking into account the agglomeration/clustering phenome-non. Therefore, the Hurricane_MK seems to be a good solution for particles with high porosity, with a tendency to agglomerate.

4.3. Hook-like curves vs. reentrainment

Often, experimental grade efficiency curves have a minima at an inter-mediate diameter (an effect that may also be present in hydrocyclones [41,42]) and as an hypothesis posed by Mothes and Löffler [34] and pursued by Paiva et al. [29] these “hook-like” curves may occur because the smaller particles agglomerate with the bigger particles, thus being captured as larger particles.

For the pilot-scale experimental cases presented in this work, the grade efficiency curves show two valleys instead of the typical one (see Figs. 5, 9 and 13). One hypothesis can be the occurrence of some degree of re-entrainment, as the constraint of the saltation velocity was partially relaxed in the optimization problem. However, for the present particle size distributions this phenomenon posed no problem in significantly reducing global collection below theoretical predictions. For the industrial case, at much higher temperature, the second valley does not occur (see Fig. 16). Since the saltation velocity increases with a decrease in gas density (refer to Eq. (11)), re-entrainment will decrease at higher temperatures, thus a higher temperature is a possible explanation for the absence of the second valley in the grade-efficiency for the industrial case.

4.4. PACyc vs. experimental results (grade efficiency curves and global efficiencies)

PACyc is not able to predict well the high efficiencies observed for the smaller particles (see Figs. 5, 9, 13 and 16) and this fact is due to CPU and memory limitations, as discussed in Paiva et al. [29].This results depend from the quality of the sampling of the inlet particle size distribution to the cyclone, of both the sub-micrometric particles and of the larger target-particles, which lead to very large sampling particle numbers, with consequent increased CPU load. There are also some extra-mechanisms that could be responsible for agglomeration/clustering of fine particles that are not considered in the model, such as electrostatic charging in the inlet conveying piping to the cyclone or fine particle screening by larger ones, but these effects, even if present, seems to be a second order effect.

The second valley that is present in the experimental grade efficiency curves was also not possible to predict, as PACyc does not quantify the effect of re-entrainment on the grade-efficiency, and further work is needed to better understand this phenomenon.

Regarding global efficiencies, PACyc predicted fairly well all cases.

5. Conclusions

The optimization that led to the Hurricane_MK cyclone was per-formed taking into account interparticle agglomeration/clustering. Experimental data obtained with very difficult dusts (very fine and porous) show that the numerically optimized Hurricane_MK is capable of quite high collection efficiencies, and, to the authors' knowledge, much higher than with any other high-efficiency cyclone, including the numerically optimized Hurricane.

PACyc predicts fairly well the global efficiencies obtained experimentally, allowing the application of this new Hurricane_MK cyclone in situations where other reverse-flow cyclones are not a solution.

Experimental data derived from three different samples with industrial relevance and a successful industrial-scale implementation show that the Hurricane_MK represents an excellent cyclone solution, currently with patent pending [38].

Nomenclature

a Height of tangential entry (m)
b Width of tangential entry (m)
C_{in} Inlet concentration (mg/m^3 or mg/Nm^3 @ 11% O_2) C_{out} Outlet concentration (mg/m^3 or mg/Nm^3 @ 11% O_2) D Cyclone diameter (m)
D_b Dust discharge diameter (m) D_e Vortex finder diameter (m)
D_{turb} Particle turbulent dispersion coefficient e Semi-angle of cyclone cone (°)
f_{obj} Objective function
g Gravity's acceleration (m/s^2)
h Height of cylindrical body (m)
H Total cyclone height (m)
k Smolik's constant
PSD Particle size distribution Q Flow rate (m^3/h)
s Vortex finder length (m)
T Temperature (°C)
u_{in} Mean entry velocity (m/s)
u_s Saltation velocity (m/s)
ΔP Pressure drop (Pa)
ΔP_{max} Maximum allowable pressure drop (Pa)
ε Particle porosity
η Global/overall efficiency $\eta_{experimental}$ Experimental global efficiency $\eta_{theoretical}$ Theoretical global efficiency
$\eta(C_1)$ Global/overall efficiency at low and know concentration
$\eta(C_2)$ Global/overall efficiency at new concentration
η_i Initial global/overall efficiency
η_{i+1} Small scale optimization problem global/overall efficiency $\eta'(i+1)$ Large scale optimization problem global/overall efficiency μ Gas viscosity (Pa·s)
ρ Fluid's density (kg/m^3)
ρ_p Particle density (kg/m^3)
ρ_{ap} Particle apparent density (kg/m^3)

References

[1] R.L. Salcedo, M.J. Pinho, Pilot- and industrial-scale experimental investigation of numerically optimized cyclones, Ind. Eng. Chem. Res. 42 (2002) 145–154.

[2] H.M. El-Batsh, Improving cyclone performance by proper selection of the exit pipe, Appl. Math. Model. 37 (2013) 5286–5303.

[3] O. Molerus, M. Gluckler, Development of a cyclone separator with new design,

Powder Technol. 86 (1996) 37–40.

[4] R.L.R. Salcedo, M.G. Candido, Global optimization of reverse-flow gas cyclones: application to small-scale cyclone design, Sep. Sci. Technol. 36 (2001) 2707–2731.

[5] G. Ramachandran, D. Leith, J. Dirgo, H. Feldman, Cyclone optimization based on a new empirical model for pressure drop, Aerosol Sci. Technol. 15 (1991) 135–148.

[6] G. Ravi, S.K. Gupta, M.B. Ray, Multiobjective optimization of cyclone separators using genetic algorithm, Ind. Chem. Eng. Res. 39 (2000) 4272–4286.

[7] G. Sun, J. Chen, M. Sci, Optimization and applications of reverse-flow cyclones, China Particuology 3 (2005) 43–46.

[8] R.L. Salcedo, J.A.G. Campos, Optimization for pollution reduction: a numerical approach to cyclone design, in: F. Friedler, J. Klemes (Eds.), 2nd Conference on Process Integration, Modeling and Optimization for Energy Saving and Pollution Reduction, Hungarian Chemical Society, 1999.

[9] R. Salcedo, J. Paiva, Pharmaceuticals: efficient cyclone systems for fine particle collection, Filtr. Sep. 47 (2010) 36–39.

[10] R.L. Salcedo, High efficiency cyclones, EP0972572A2, European Patent Application 99670006.8, Bulletin 2000103, January 19, 2000.

[11] F.A. Zenz, Cyclone-design tips, Chem. Eng. 108 (2001) 60–64.

[12] W. Licht, Air Pollution Control Engineering — Basic Calculations for Particulate Collection, Marcel Dekker, New York and Basel, Switzerland, 1980.

[13] W.L. Heumann, Cyclone separators: a family affair, Chem. Eng. (1991) 118–123.

[14] C.E. Lapple, Processes use many collector types, Chem. Eng. 58 (1951) 144–151.

[15] J. Dirgo, D. Leith, Cyclone collection efficiency: comparison of experimental results with theoretical predictions, Aerosol Sci. Technol. 4 (1985) 401–415.

[16] I. Karagoz, A. Avci, A. Surmen, O. Sendogan, Design and performance evaluation of a new cyclone separator, J. Aerosol Sci. 59 (2003) 57–64.

[17] P. Schmidt, Unconventional cyclone separators, Int. Chem. Eng. 33 (1993) 8–17.

[18] R.L. Salcedo, Solving non-convex NLP and MINLP problems with adaptive random-search, Ind. Eng. Chem. Res. 31 (1992).

[19] H. Mothes, F. Löffler, Prediction of particle removal in cyclone separators, Int. Chem. Eng. 28 (1988) 231.

[20] R.L. Salcedo, Solving non-convex NLP and MINLP problems with adaptive random-search, Ind. Eng. Chem. Res. 31 (1992) 262–273.

[21] R. Lima, R.L. Salcedo, D. Barbosa, SIMOP-efficient reactive distillation optimization using stochastic optimizers, Chem. Eng. Sci. 61 (2006) 2006.

[22] H.G. Silva, R.L. Salcedo, SIMOP: application to MINLP stochastic optimization, Chem. Eng. Sci. 66 (2011) 1306–1321.

[23] C.B. Shepherd, C.E. Lapple, Flow pattern and pressure drop in cyclone dust collectors cyclone without intel vane, Ind. Eng. Chem. 32 (1940) 1246–1248.

[24] K.J. Caplan, 43 — source control by centrifugal force and gravity, in: A.C. Stern (Ed.), Sources of Air Pollution and Their Control, Second Edition Academic Press, 1968, pp. 359–407.

[25] M. Bohnet, T. Lorenz, Separation efficiency and pressure drop of cyclones at high temperatures, in: R. Clift, J.P.K. Seville (Eds.), Gas Cleaning at High Temperatures, Springer, Netherlands, 1993, pp. 17–31.

[26] W. Barth, Berechnung und Auslegung von Zyklonabscheidern auf Grund neuerer Untersuchungen, Bund der Ingenieure für Wasserwirtschaft, Abfallwirtschaft und Kulkurbau, 81956. 1–9.

[27] C.J. Stairmand, Pressure drop in cyclone separators, 1949. 409–412.

[28] E. Muschelknautz, Auslegung von Zyklonabscheidern in der technischen Praxis, Staub Reinhalt. Luft 30 (1970) 187–195.

[29] J. Paiva, R. Salcedo, P. Araujo, Impact of particle agglomeration in cyclones, Chem. Eng. J. 162 (2010) 861–876.

[30] R.M. Alexander, Fundamentals of cyclone design and operation, Proc. Aus. Inst. Min. Met. 152 (1949) 152–153.

[31] R.L. Salcedo, M.A. Coelho, Turbulent dispersion coefficients in cyclone flow: an empirical approach, Can. J. Chem. Eng. 77 (1999) 609–617.

[32] R.L.R. Salcedo, V.G. Chibante, A.M. Fonseca, G. Cândido, Fine particle capture in biomass boilers with recirculating gas cyclones: theory and practice, Powder Technol. 172 (2007) 89–98.

[33] V.G. Chibante, A.M. Fonseca, R.R. Salcedo, Comparing the performance of recirculating cyclones applied to the dry scrubbing of gaseous HCl with hydrated lime, Ind. Eng. Chem. Res. 48 (2008) 1029–1035.

[34] H. Mothes, F. Löffler, Zum einflub der partikelagglomeration auf die abschiedung im gaszyklon, Staub Reinhalt. Luft 44 (1984) 9–14.

[35] C.A. Ho, M. Sommerfeld, Modelling of micro-particle agglomeration in turbulent flows, Chem. Eng. Sci. 57 (2002) 3073–3084.

[36] G. Gronald, G. Staudinger, Investigations on Agglomeration in Gas Cyclones, , 2006.

[37] J. Chen, M. Shi, A universal model to calculate cyclone pressure drop, Powder Technol. 171 (2007) 184–191.

[38] R. Salcedo, J. Paiva, Ciclone Aglomerador de fluxo invertido e respetivo processo, PAT 107312, INPI, November 25, 2013.

[39] C.W. Haig, A. Hursthouse, S. McIlwain, D. Sykes, The effect of particle agglomeration and attrition on the separation efficiency of a Stairmand cyclone, Powder Technol. 258 (2014) 110–124.

[40] L. Svarovsky, J. Williams, T. Allen, Handbook of powder technology, Handbook of Powder Technology, Elsevier Science B.V., 1981, p. ii.

[41] W. Chen, N. Zydek, F. Parma, Evaluation of hydrocyclone models for practical application, Chem. Eng. J. 80 (2000) 295–303.

[42] W. Wang, P. Zhang, L. Wang, G. Chen, J. Li, X. Li, Structure and performance of the circumfluent cyclone, Powder Technol. 200 (2010) 158–163.